A Review on Machine Topologies and Control Techniques for Low-Noise Switched Reluctance Motors in Electric Vehicle Applications

CHUN GAN[1,2], **(Member, IEEE), JIANHUA WU**[2], **QINGGUO SUN**[2],
WUBIN KONG[3], **(Member, IEEE), HONGYU LI**[1,4], **(Student Member, IEEE),**
AND YIHUA HU[5], **(Senior Member, IEEE)**

[1]Department of Electrical Engineering and Computer Science, The University of Tennessee, Knoxville, TN 37996, USA
[2]College of Electrical Engineering, Zhejiang University, Hangzhou 310027, China
[3]School of Electrical and Electronic Engineering, Huazhong University of Science and Technology, Wuhan 430074, China
[4]College of Energy and Electrical Engineering, Hohai University, Nanjing 211100, China
[5]Department of Electronic and Electrical Engineering, University of Liverpool, Liverpool L69 3BX, U.K.

Corresponding author: Jianhua Wu (hzjhwu@163.com)

ABSTRACT This paper presents a technical overview for low-noise switched reluctance motor (SRM) drives in electric vehicle (EV) applications. With ever-increasing concerns over environmental and cost issues associated with permanent magnet machines, there is a technical trend to utilize SRMs in some mass production markets. The SRM is gaining much interest for EVs due to its rare-earth-free characteristic and excellent performance. In spite of many advantages compared with conventional adjustable-speed drives, SRMs suffer from torque ripple and radial distortion (and thus noise and vibration) by their nature. Therefore, for high-performance vehicle applications, it is important and urgent to optimize the SRM system to overcome the drawbacks of the noise and vibration. In order to present clear solutions to the acoustic noise in SRMs, this paper starts by analyzing the mechanism of the radial vibration and torque ripples inherent in the motors, and then focuses on the state-of-the-art technologies to mitigate the radial force and torque ripples. It highlights two categories for low-noise SRMs, including the machine topology improvement and control strategy design for radial vibration mitigation and torque ripple reduction. Advanced technologies are reviewed, classified, and compared accordingly. In addition to these methodologies, the schemes that have been developed by authors are also presented and discussed. Finally, the research status on this topic is summarized and forecast research hotspots are presented. It is our intention that this paper provides the guidance on performance improvements for low-noise SRM drives in EV applications.

INDEX TERMS Switched reluctance motor (SRM), low noise, torque ripple, radial distortion, control, motor structure.

I. INTRODUCTION

Electric vehicle (EVs) and hybrid EVs have been attracting much attention due to the high demand of fuel efficiency and environmental protection against air pollution [1], [2]. Permanent magnet synchronous motors (PMSMs) are popular for EV and hybrid EV applications [3]–[5]. However, these motors rely on permanent magnets, which are made from rare-earth materials. High cost, limited reserve, and environmental impact associated with extracting and refining rare-earth materials limit their applications in mass EV markets. Furthermore, the sensitivity of permanent magnets to high temperature compromises the motor performance in harsh automotive environments. Hence, there is an increasing need to develop rare-earth-free motors for high-performance EV applications [6], [7].

Among competing for motor technologies, switched reluctance motors (SRMs) have received growing attention for both industry and research community due to the rare-earth-free characteristic and excellent performance [8]–[21]. Their advantages include simple structure, low cost, robust configuration, and fault tolerance ability, making them suitable for high-speed, high-temperature, and safety-critical applications, such as EV/HEV [8]–[18], aircraft [19], and home appliances [20], [21]. Although there are many advantages

compared to traditional AC machines, the acoustic noise resulting from the radial vibration and torque ripple is an inherent disadvantage in SRMs. This source of noise needs to be mitigated if the motor is employed for a high-performance EV application. Hence, it is important and urgent to optimize the SRM system to solve the vibration and torque ripple issues. In order to present clear solutions to the acoustic noise in SRMs, this paper focuses on reviewing the state-of-the-art technologies to mitigate both the radial force and torque ripple, mainly following two categories, including the motor topology improvement and control strategy design. Advanced technologies including the authors' contribution in this research area are reviewed, classified, and analyzed in details. Furthermore, these methods are summarized and compared in terms of adopted methods, advantages, and limitations.

In SRMs, the electromagnetic attraction force can be divided into two components, including the tangential force and radial force with respect to the rotor. The tangential force contributes to the output torque and its variation causes the torque ripple; the radial force leads to vibration and frame deformation. Therefore, to achieve a low-noise SRM drive, both the torque ripple and radial vibration should be reduced. Many advanced technologies have been proposed in the literature. Fig. 1 shows the classification of possible improvements on the radial force and tangential force for the developments of motor topologies and control strategies, which will be analyzed in details in the following sections.
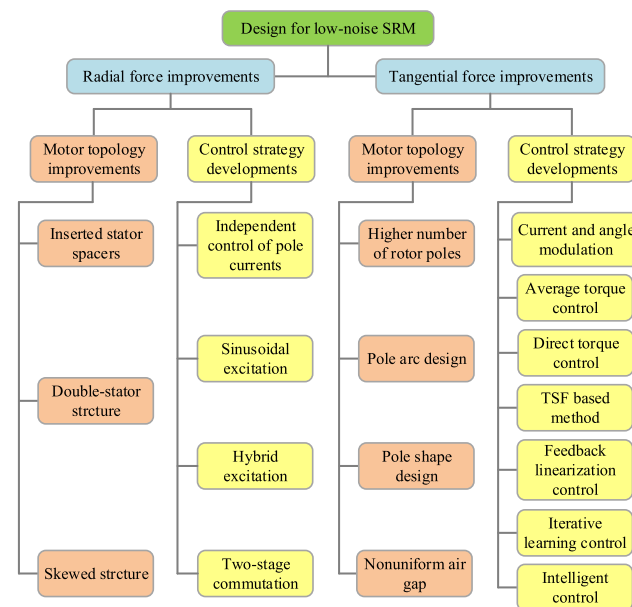

FIGURE 1. Classification of possible developments for low-noise SRM drives.

II. SRM DRIVE AND ELECTROMAGNETIC FORCE

Fig. 2(a) shows a typical three-phase 12/8-pole SRM drive, where the conventional asymmetric half-bridge converter is used to drive the motor. The converter provides phase isolation and fault-tolerance ability. If one phase leg fails,
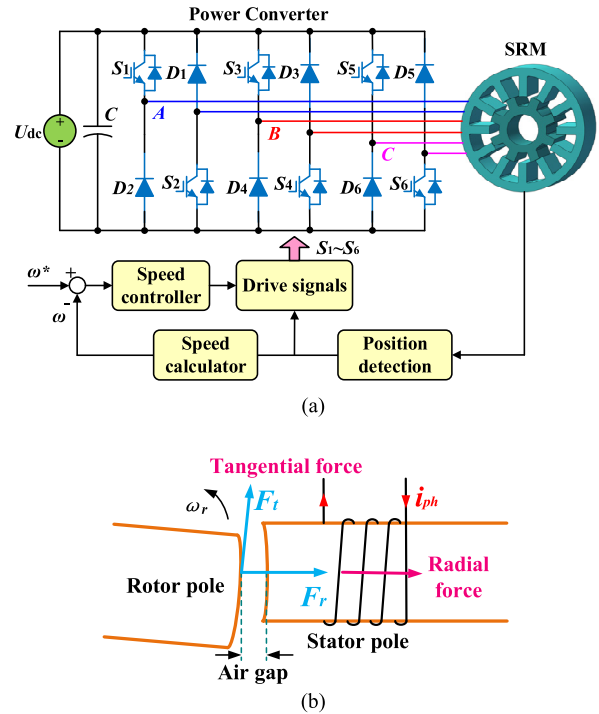

FIGURE 2. SRM drive and attraction force. (a) Three-phase SRM drive. (b) Attraction force produced by stator and rotor poles.

other ones can still operate normally to produce a continuous torque. The electromagnetic attraction force of the SRM is illustrated in Fig. 2(b). When a current flows in the phase winding, the attraction force on the rotor is generated, which can be separated into the tangential force and radial force. The tangential force converts into the torque and the radial force leads to the vibration on the stator frame.

The voltage equation for one phase can be expressed as

$$U_k = R_k i_k + L_k(\theta)\frac{di_k}{dt} + i_k\omega\frac{dL_k(\theta)}{d\theta} \quad (1)$$

where U_k is the phase voltage, R_k is the phase resistance, L_k is the phase inductance, i_k is the phase current, ω is the motor angular speed, and θ is the rotor position.

The tangential force density and radial force density in the air gap are given by

$$f_t = \frac{1}{2\mu_0}2B_r B_t \quad (2)$$

$$f_r = \frac{1}{2\mu_0}(B_r^2 - B_t^2) \quad (3)$$

where μ_0 is the relative permeability of vacuum, f_t and f_r are the tangential and radial force densities, respectively; B_t and B_r are the tangential and radial magnetic flux intensities from the tangential and vertical directions, respectively.

The tangential and radial forces in an integral surface can be obtained from (2) and (3), by

$$F_t = \int_s f_t ds = \frac{1}{\mu_0}\int_s B_r B_t ds \quad (4)$$

$$F_r = \int_s f_r ds = \frac{1}{2\mu_0}\int_s (B_r^2 - B_t^2)ds \quad (5)$$

The torque acting on the rotor pole can be derived by

$$T_t = F_t \frac{D_{ro}}{2} = \frac{D_{ro}}{2} \int_s f_t ds = \frac{D_{ro}}{2\mu_0} \int_s B_r B_t ds \quad (6)$$

where T_t is the torque and D_{ro} is the rotor outer diameter.

III. RADIAL VIBRATION MITIGATION STRATEGIES

Acoustic noise caused by the radial force is an inherent characteristic in SRMs. Due to the rapid change of the electromagnetic force during the phase commutation, the radial vibration of the stator is a significant source of the acoustic noise. Hence, to obtain a low-noise SRM, the radial force and vibration can be mitigated by employing proper strategies.

A. CALCULATION OF RADIAL FORCE AND VIBRATION

In [22], the origin of the vibration in SRMs is investigated and an analytical model for the vibration is developed based on the mechanical impulse response of the stator frame. A fast and precise acoustic noise imaging scheme for SRMs is conducted in [23], based on the distribution of the radial vibration in the stator frame, which is computed by using the phase current and phase voltage. In [24] and [25], an analytical relationship between the radial force and vibration is investigated, which can be used to predict the noise at different operation frequencies. Furthermore, a detailed analytical model for the radial force calculation is presented. A simulation model to predict the transient vibration for SRMs is developed under different operating conditions [26], such as startup, load change, and braking. This vibration prediction model is derived from the phase current and a rotor position based look-up table using the finite-element method. A fast radial vibration calculation method for SRM is presented in [27], based on the current and its slope.

B. MOTOR TOPOLOGY DEVELOPMENTS

In [28], the traditional slot wedges in SRMs are exchanged by structural stator spacers, which are made of stiff nonmagnetic materials (preferably ceramics). Fig. 3 shows the stator structure with and without structural stator spacers in a four-phase 8/6-pole SRM. This modification to the stator laminations can reduce the vibration and secure the windings. A simple design of a cylindrical rotor is proposed in [29], by connecting
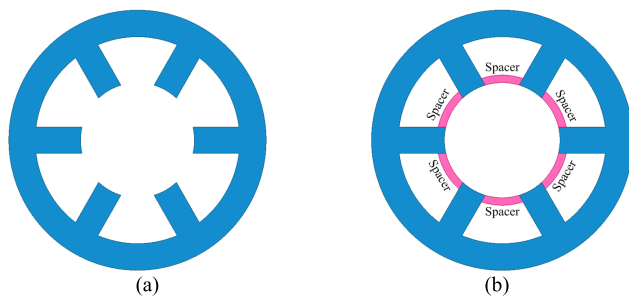
the salient poles with thin ribs, to reduce the acoustic noise at high rotational speeds. An investigation of vibration and acoustic noise is presented in [30] by analyzing the material and structure of the stator frame, and an optimization method on the motor structure is provided. In [31], acoustic noise reduction by designing frame thicknesses and shapes are investigated for high-speed SRMs.
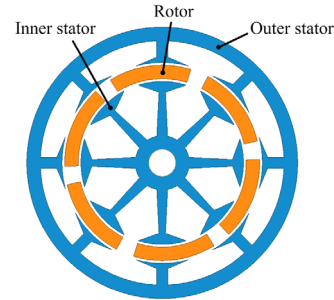

FIGURE 4. Double stator SRM structure [32], [33].

Compared to the conventional motor structure, a double-stator SRM (DSSRM) is proposed to reduce the radial forces in machines [32], [33], as shown in Fig. 4. The rotor is assembled between the inner stator and outer stator, and the attraction force is generated on the rotor pole from the inner and outer stators. The double-stator configuration and magnetic force of the DSSRM are analyzed in details in [32]. The structural behavior of a DSSRM and a conventional SRM is compared in [33], by using multi-physic analysis, which illustrates an obvious reduction in vibration.

The stator and rotor poles of SRMs can also be improved to reduce the radial force. A single-phase SRM by skewing the stator and rotor poles is developed in [34], and the acoustic noise and vibration are investigated and compared under different skewing angles. From this work, it can be seen that proper skewing can effectively mitigate the acoustic noise and vibration for SRMs. The skewing technology is also employed for linear SRMs in [35], and the optimal skewing angle is investigated by using the finite element method (FEM). In [36], skewing effects on both stator and rotor poles for a three-phase 12/8 SRM are investigated by the authors, and the motor structure is illustrated in Fig. 5. Different skewing technologies are presented, and the radial force, torque, and efficiency are compared in details. From the results, it can be concluded that skewing the stator pole is a more effective way to reduce the SRM vibration than skewing the rotor pole.

C. CONTROL STRATEGY IMPROVEMENTS

1) INDEPENDENT CONTROL OF POLE CURRENTS

As illustrated in Fig. 6(a), a phase winding for a three-phase 12/8-pole SRM is composed of four pole windings, i.e., A_1, A_2, A_3, and A_4, which is connected in series. The radial force and torque can be separately controlled when all the pole currents are independently controlled, as shown in Fig. 6(b). In [37], a controlled radial force scheme is

FIGURE 3. Stator structure with and without structural stator spacers. (a) Conventional stator. (b) Developed stator [28].

FIGURE 5. Skewed motor structure [36]. (a) Skewed stator. (b) Skewed rotor.
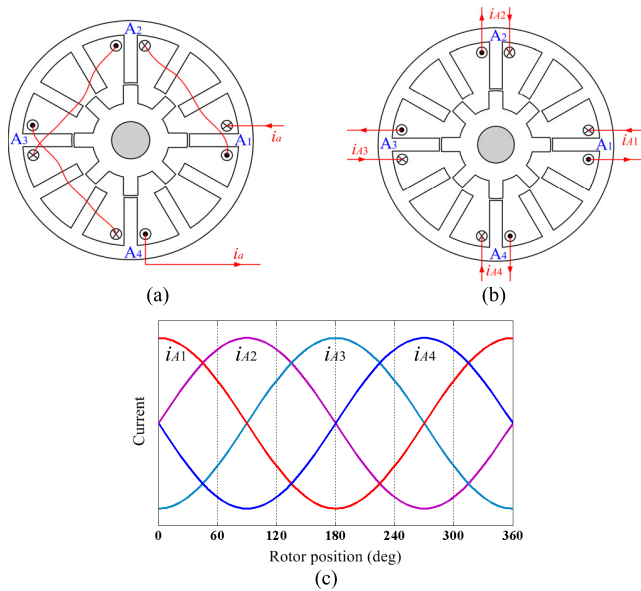

FIGURE 6. Independently controlled pole currents. (a) Series pole windings. (b) Independent pole windings [37]. (c) Sinusoidal excitations [38].

proposed. In this scheme, the torque is controlled by the traditional method, i.e., the same current is applied to all the poles in the excited phase to produce the desired torque. Two additional poles from the descending-inductance phase are energized to generate the desired radial force. However, the negative torque will generate in this case, and some torque produced by other poles will be cancelled out. In [38], a sinusoidal current excitation method is presented for the radial force control of SRMs based on the independent control of pole currents, as shown in Fig. 6(c). By employing the selected sinusoidal currents, the radial force can be reduced and the required rotational torque can be generated. However, a large number of power switches is needed, which compromises the system efficiency.

2) HYBRID EXCITATION
A hybrid excitation method for SRM is proposed in [39] to reduce the radial vibration force and acoustic noise. The motor is excited by combining one-phase excitation and two-phase excitation. In the torque generation region, the next

phase is excited before the turn-off angle of the previous phase, and thus a low vibration can be achieved in the overlapped excitation region. In [40], the average torque and radial force are independently controlled with hybrid excitation.

3) TWO-STAGE COMMUTATION
In asymmetric half-bridge converters, the upper switch and lower switch are both turned off in the non-conduction region, and the current goes back to the power supply quickly under a negative bus voltage, where recovering energy to the power supply is achieved. However, it causes a vibration in the phase commutation region. Therefore, a two-stage commutation strategy is proposed in [41]–[43], where a zero-voltage loop is employed in the control algorithm during the phase commutation region, as presented in Fig. 7. When the current reaches the turn-off angle, the upper switch is turned off and the lower switch remains on instead of turning off compared to the conventional scheme. In this state, the current flows through the lower switch and lower diode in a zero-voltage loop. Then, the lower switch is turned off, and the current flows back to the power source. There are two stages in the phase commutation region including zero-voltage loop and negative voltage stages.
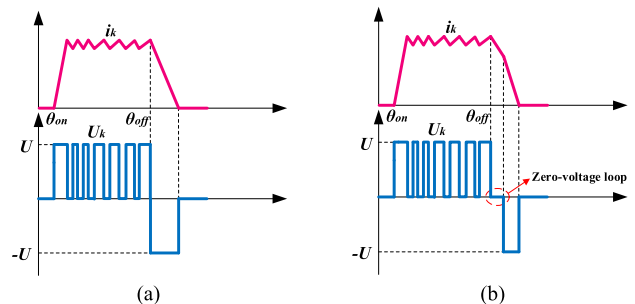

FIGURE 7. Phase current and phase voltage. (a) One-stage commutation. (b) Two-stage commutation.

D. COMPARISON OF RADIAL VIBRATION MITIGATION TECHNIQUES
The comparison of existing radial vibration mitigation techniques is illustrated in Table 1. The above-mentioned motor topology design methods and control strategies are summarized in terms of adopted techniques, advantages, and disadvantages. Although advanced techniques can be used to mitigate the radial vibration, each method has its own limitations. As illustrated in the table, the first three methods focus on motor topology improvements, and others on control scheme improvements.

The inserted stator spacers, DSSRM, and skewed poles all bring the complexity to the motor structure. The skewing technique is usually used in the reduction of radial vibration in SRMs. The skewed motors can be designed with different phases and power levels, and can be controlled easily by conventional control schemes. Compared to the

TABLE 1. Summary and comparison of radial vibration mitigation techniques.

Method	Adopted technique	Advantage	Disadvantage	Reference
Inserted stator spacers	Replace the slot wedges with structural stator spacers	Reduced radial vibration; reduced windage losses; robust structure; small modifications in stator laminations	Complicated fabrication; difficult installation	[28]
Cylindrical rotor	Connect salient rotor poles with thin ribs	Reduced radial vibration; reduced windage losses; improved efficiency	Thin rib causes deformation at high rotational speed	[29]
DSSRM	Assemble the rotor between the inner stator and outer stator	Reduced radial vibration; high power density	High cost for motor prototype; complicated motor structure	[32], [33]
Skewed poles	Skew the stator and rotor poles with proper angles	Reduced radial vibration; controlled with conventional schemes	Complicated fabrication with different stacks between two laminations	[34]-[36]
Independent control of poles currents	Each pole winding is independently connected; two additional poles are energized to produce the desired radial force	Radial force and torque can be controlled independently; the desired radial force can be achieved	High cost for more used switching devices; produce negative torque; lower system efficiency	[37], [38]
Hybrid excitation	Combine one-phase excitation and two-phase excitation	Noise and vibration are reduced by hybrid excitation; high efficiency; short tail current; easy to implement	Poor fault-tolerant ability due to the use of C-dump converter circuit	[39], [40]
Two-stage commutation	Add a zero-voltage loop when the corresponding phase is turned off	Reduced radial vibration; easy to implement	Increased tail current; easily generate negative torque; reduced torque ability	[41]-[43]

motor topology design, improved control strategies are much easier to implement. Although the independent control of the pole current can reduce the radial force, a large number of power switches is required, which increases the cost of the motor drive. The hybrid excitation and two-stage commutation control schemes are derived from the conventional control schemes, such as current regulation control, voltage-PWM control, and angle modulation control, and thus easy to implement. However, for the two-stage commutation scheme, the tail current leads to negative torque generation. Therefore, a proper angle selection for the two-stage commutation is important for the motor performance improvement.

IV. TORQUE RIPPLE REDUCTION TECHNOLOGIES
In SRMs, a high torque ripple will also lead to acoustic noise, which will affect the control performance in a closed-loop system. Many advanced technologies have been put forward to reduce the torque ripple, including the motor topology development and control strategy improvement.

A. MOTOR TOPOLOGY DEVELOPMENTS
SRMs are typically designed with the symmetrical and evenly distributed stator and rotor poles around the circumference. They are expected to produce continuous and smooth torque. Over the past years, some SRM configurations with various numbers of stator and rotor poles have been proposed in [44]–[47]. A summary of known motor configurations with accepted number of stator and rotor poles is given as follows [44], [47]: three-phase SRMs: 6/2, 6/4, 6/8, 6/14, 12/8, 18/12, and 24/16; four-phase SRMs: 8/6, 8/10, 16/12, 24/18, and 32/24; five-phase SRMs: 10/4, 10/6, 10/8, and

10/12; six-phase SRMs: 12/10, 12/14, and 24/20; seven-phase SRMs: 14/10, 14/12, and 14/16.

In [44], a low-power 6/10-pole SRM is developed and compared with a traditional 6/4-pole motor. The work shows that a higher rotor number based SRM can provide lower torque ripple in the non-saturation condition. However, it produces a higher torque ripple compared to the 6/4 SRM in the saturation condition. Clearly, there is a tradeoff between the high torque and low torque ripple with a higher current excitation. Through optimizing the phase number, it is possible to improve the torque with a lower ripple. Conventionally, the arc angle of the rotor pole is slightly larger than the arc angle of the stator pole in the SRM. Therefore, to obtain a more compact SRM with smooth torque production, the relationship between the arc angles of the stator pole and rotor pole is considered in [45]. Stator pole and rotor pole combination, winding connection, and electromagnetic performance of a new variable flux reluctance machine, which is similar to SRMs, are investigated in [46], and the static torque and torque ripple are compared among different pole number combinations.

Some other strategies focus on the development of stator and rotor pole shapes to reduce the torque ripple, as shown in Fig. 8. Optimized stator and rotor pole arcs (see Fig. 8(a)) of an 8/6-pole SRM are obtained by FEM analysis, where the average torque is improved and the torque ripple is reduced [48]. The geometry for low torque ripple SRMs is investigated in [49] and a motor having notched poles (see Fig. 8(b)) is proposed by FEM analysis. Compared to the conventional motor structure, the torque ripple is reduced by 4.4%. An 8/6-pole SRM having slant pole face shapes (see Fig. 8(c)) is presented in [50], where the slant is designed
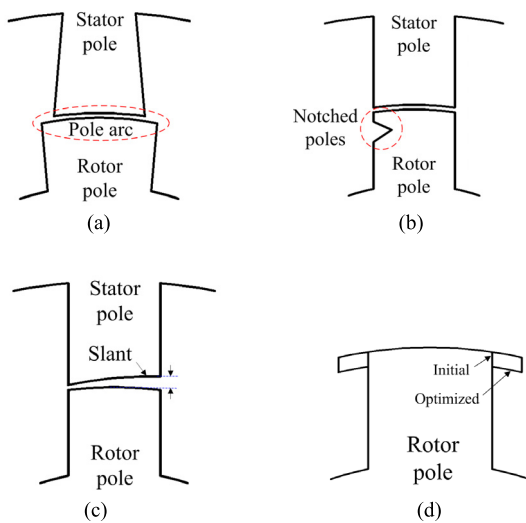
FIGURE 8. Motor pole improvements. (a) Pole arc [48]. (b) Rotor pole notch [49]. (c) Stator pole slant [50]. (d) Rotor pole shoe [51].

FIGURE 9. Rotor face design for uniform air gap [48]. (a) Uniform air gap. (b) Nonuniform air gap [55].

in the stator pole including two cases. In the first case, the air gap decreases when the rotor pole approaches the fully aligned position; in the second one, the air gap increases when the stator and rotor poles tend to overlap. A pole shoe attached to the lateral face of the rotor pole is presented in [51], as shown in Fig. 8(d). The design parameters are optimized, where the average torque is improved and the undesired torque ripple is minimized by this additional optimization. In [52], stator pole height, stator taper angle, rotor pole arc, and pole shoe shape are all optimized in a three-phase 24/16-pole SRM to minimize the torque ripple and improve the torque ability for traction applications.

A method by inserting a notched hole in each rotor pole is presented in [53] for torque ripple reduction in a mutually coupled SRM, which is similar to the case in Fig. 8(b). The average torque and torque ripple are investigated accordingly. From this work, similar average torque can be produced with these punching holes, and the torque ripple is much lower than the motor without these holes. A method by applying the relocation of rotor molding clinches is presented in [54]. The mitigation effects of the torque ripple in short-pitched SRMs and fully-pitched SRMs are both analyzed and compared. The torque ripples of the two motors are lower when molding pins are closed to the rotor pole head. A nonuniform air gap is considered in [55] for a flat torque production with a lower torque ripple in a high-speed two-phase 4/2-pole SRM, as shown in Fig. 9.

B. CONTROL STRATEGY IMPROVEMENTS

According to the operation principle of SRMs, the inductance gradients in the minimum and maximum inductance regions are both very small. Therefore, the generated phase torque is very low in these regions, which will cause a torque decline in the phase commutation region, leading to the torque ripple. Compared to the schemes of motor topology design to reduce
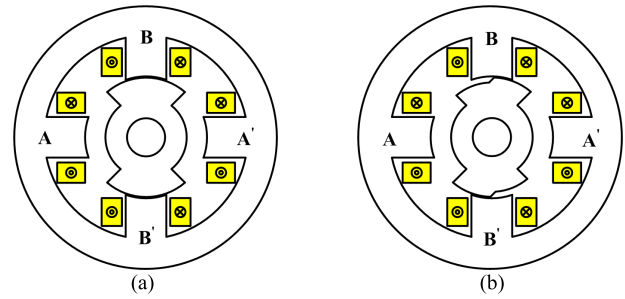
the torque ripple, control technique improvements are easier and more cost-effective to implement.

1) CURRENT AND ANGLE MODULATIONS

Conventionally, there are two control schemes to reduce the torque in SRMs, including the angle optimization method [56]–[58] and current profiling method [59]–[63]. The turn-on and turn-off angles are optimized to lower the torque ripple in [57] and [58], and a new method utilizing online calculations of the optimal angles is proposed. However, the phase current and torque cannot be flexibly controlled at the desired reference. A new current controller is proposed in [59] to accurately track the reference current to minimize the torque ripple in SRMs. By using the proposed scheme, the torque ripple can be reduced to 5%. Modulation of phase current profiles is focused in [60]–[62] to generate a smooth torque. However, a large amount of memory is required to store the current profiles for the current profiling method. A high-performance current controller for SRM drives based on the online estimated parameters by current profiling method is proposed in [63] to reduce the torque ripple. Additionally, the torque ripple can also be reduced by the independent control of pole currents, which is similar to the method in Fig. 9 [37], [38].

2) ATC AND DTC

A new torque controlled scheme to estimate and control the average torque of SRMs is proposed in [64], and the diagram is shown in Fig. 10(a). The average torque control (ATC) strategy can be implemented by using this online average torque and energy ratio estimation method for the closed-loop control. The torque reference is continuously adjusted by changing the switching angles and current reference to maintain a constant average torque at a given reference. Due to the adaptive adjustment of the system parameters, high accuracy of torque estimation is obtained and precise torque control can be carried out. Therefore, the torque ripple can be suppressed at an accepted level.

Direct torque control (DTC) techniques have been employed and designed to minimize the torque ripple for SRMs [65]–[67], and the diagram is illustrated in Fig. 10(b). The current reference is calculated from current profiles
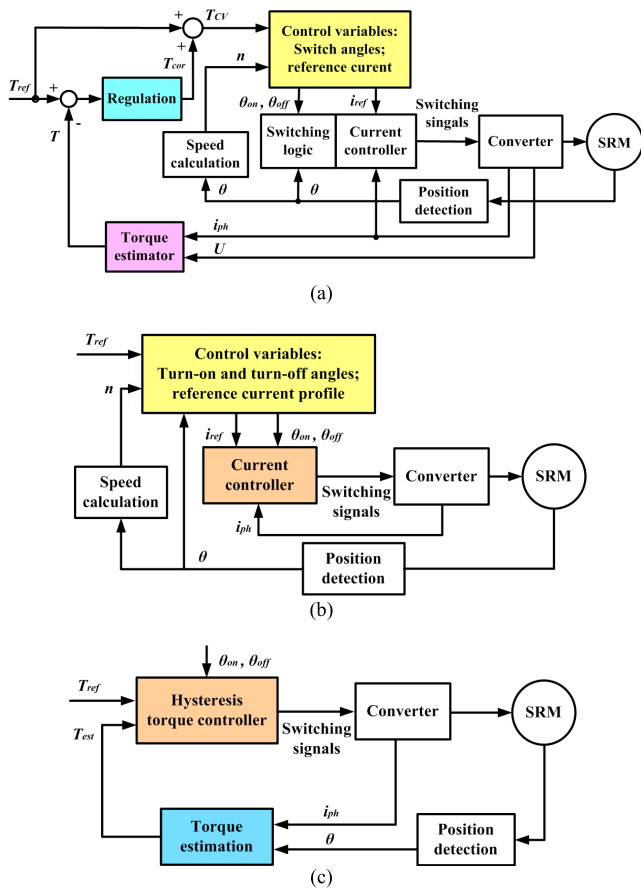
FIGURE 10. Block diagram of torque control scheme. (a) ATC [64]. (b) DTC. (c) DITC [68].

stored in the look-up table including the current-torque-position (i-T-θ) characteristic. Switching signals are obtained from the current controller by comparing the sampled currents and reference currents. The direct instantaneous torque control (DITC) is derived from the DTC, which has attracted more interest due to its rapid response to the torque error, and thus the torque ripple can be reduced more effectively [68], [69]. The diagram of the DITC is illustrated in Fig. 10(c). The torque reference is directly used for control without transforming into current reference. The instantaneous torque is estimated online, which is directly employed as the control variable without any current loop. Switching signals are generated by a torque hysteresis controller. An approach by employing the DITC to simultaneously eliminate the torque ripple and vibration of SRMs is proposed in [70], achieving a high-performance motor system for automotive applications.

Another instantaneous torque control method is proposed in [71] by regulating the associated co-energy of the SRM which is estimated according to the voltage, current, and inductance to follow a co-energy profile. In [72], a Lyapunov function based robust direct torque controller is reported for torque ripple minimization. The proposed controller is capable of handling the nonlinear torque production

mechanism for the SRM, which is also shown to be robust in the presence of uncertainties in the flux-linkage model.

3) TSF BASED CONTROL

To reduce the torque ripple for SRMs, the torque sharing function (TSF) with current hysteresis control is usually employed. The torque reference of each phase can be defined by a TSF, where the sum of the phase torque references is equal to the output torque reference. The phase torque can be obtained from the predefined torque profile in a look-up table including the i-T-θ characteristic. Fig. 11(a) presents the linear and sinusoidal TSF profiles for the three-phase SRM [73]. In the two-phase commutation region, the torque references of the next phase and previous phase rise to the total torque reference and decrease to zero, respectively. The total torque reference is constant, which is the sum of the phase torque references. Therefore, by using the TSF, the output torque can be controlled with a low torque ripple.
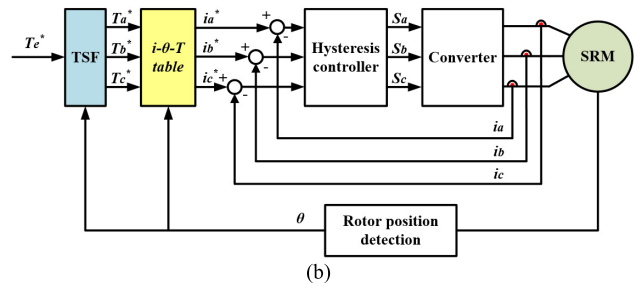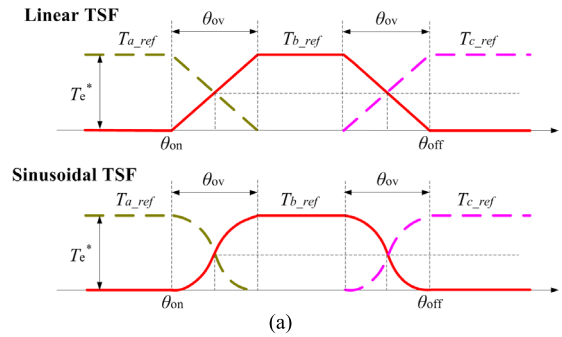

FIGURE 11. TSF-based torque control scheme. (a) Profiles of linear and sinusoidal TSFs. (b) Block diagram of TSF based torque control scheme.

Fig. 11(b) shows the TSF-based torque control diagram for conventional three-phase SRMs. The total torque reference T_e^* is divided into phase torque references T_a^*, T_b^*, T_c^* through the TSF according to the rotor position. Phase current references i_a^*, i_b^*, i_c^* are all obtained from the i-T-θ table, where the phase torque references and actual rotor position are the inputs. The actual phase currents are compared with their current references in the current hysteresis controller to generate switching signals for the converter.

The torque of the traditional current-chopping control (CCC) system and TSF-based torque control system is compared in Fig. 12, by modeling a 12/8 SRM drive in Matlab/Simulink. The phase torque references are defined
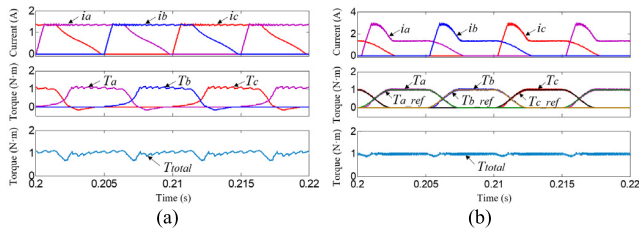
FIGURE 12. Torque comparison between CCC and TSF methods. (a) CCC method. (b) TSF method.

by using the sinusoidal TSF. The motor parameters are set to be the same and the load is set to 1 N · m. Fig. 12(a) presents the simulation results for the CCC system. There is a large torque ripple in the phase commutation region because of the insufficient torque generated by the next conducted phase in the commutation region. To solve the torque ripple issue, the TSF method is adopted by employing a current hysteresis controller to track the torque references. As shown in Fig. 12(b), the next phase currents in the commutation regions are increased and the instantaneous phase torques track the references well. The output torque is smoother and the torque ripple is significantly reduced compared to that in the CCC system.

By employing the TSF method, the phase currents change smoothly avoiding large peak currents. In the phase commutation region, the next and previous phases should be carefully controlled, and thus a reasonable TSF should be selected and defined for the optimal torque controller. To achieve lower torque ripple and better performance, many advanced techniques have focused on TSF design and improvements.

The TSF concerned with copper losses minimization and drive performance maximization are presented in [73]. The features and satisfied TSFs are analyzed in [74], based on the static torque characteristics of the prototype motor. The conventional TSF is only defined in the positive torque region, causing a poor torque performance at high speeds, due to the delay of the current rising and falling. To solve this problem, the defined region of the TSF is extended to the negative torque region in [75]. By using a new nonlinear TSF defined in [76], the currents of two adjacent phases in the commutation region can be flexibly controlled, where the efficiency is enhanced and the torque ripple is reduced. Two improved TSFs including sinusoidal and exponential TSFs are presented in [77], by optimizing the turn-on angle and overlapped angle of the TSF at various torque demands. Instantaneous torque control for SRMs is achieved by a proposed multiphase torque-sharing method in [78]. However, the scheme requires accurate information on motor characteristics. In order to compensate the torque error generated by imperfect phase current tracking, a compensator is added to the TSF in [79], where the extended speed, high average torque, and low torque ripple are all achieved. An offline TSF for SRM drives is described in [80], and the torque ripple can be significantly reduced over a wide

speed range. In [81], an online TSF compensation method is proposed by the authors to minimize the torque ripple in SRMs, where the positive and negative compensations are employed for the outgoing and incoming phases, respectively.

4) FEEDBACK LINEARIZATION CONTROL

Feedback linearization (FBL) control algorithm utilizes a state feedback to the nonlinear system to linearize the closed-loop system.FBL control for SRMs is first introduced in [82], which effectively compensates the nonlinear characteristics of the motor. The block diagram of the FBL control is illustrated in Fig. 13. A linear controller can be used by transforming the nonlinear system into a linear system, providing a required decoupling among currents. The motor characteristics and control parameters including the position, speed, and current should be accurately obtained.
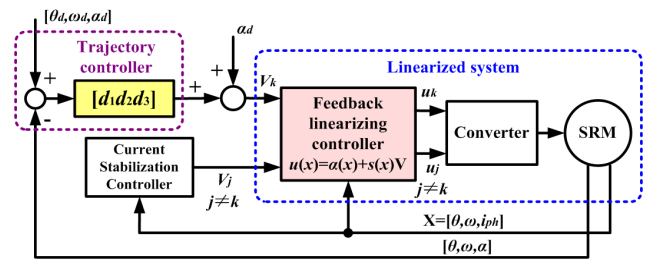

FIGURE 13. Block diagram of FBL control system [82].

The design of a robust FBL controller based on Lyapunov's second method is proposed in [83] to reduce the torque ripple in the motor drive. It takes care of uncertain model to ensure a good speed tracking ability and stability for a robust system. Adaptive nonlinear control is investigated in low-speed and high-torque operations in [84]. A simple dynamic model for the motor system is proposed by using *B* splines and a set of Fourier basis functions. Adaptive FBL controller is designed based on this model, which is simple, quick, and easy to implement. However, the disadvantage is that a large number of parameters leads to poor transient performance. An FBL current controller, which linearizes and decouples the current control loop, is presented in [85] for both low- and high-speed operations.

5) ITERATIVE LEARNING CONTROL

Iterative learning control (ILC) is especially suited for nonlinear, highly coupled, and high-precision model analysis without the need to identify the system parameters. Therefore, it is considered for dynamic torque control of SRMs to reduce the torque ripple. In [86], the ILC is developed following two steps to deal with the torque control in SRMs, including the determination of appropriate phase current waveforms for specified torques and the suitable phase voltages for faithful tracking of these waveforms. Fig. 14 shows the iterative learning of the feed-forward compensator for the torque control of SRMs. A novel ILC-based current controller for SRM drives is proposed to reduce the torque ripple
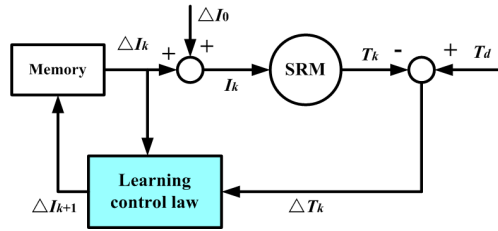
FIGURE 14. Block diagram of iterative learning control [86].

FIGURE 16. Block diagram of torque ripple compensation scheme [91].

without the requirement of the accurate motor model, where the perfect current tracking can be achieved in different operating states [87]. Conventionally, phase current references obtained from the torque function lead to torque error. For a constant output torque, the error in the phase current reference will appear periodically with respect to the rotor position. To deal with this issue, ILC is employed to compensate the phase current reference in [88] to eliminate the torque error when entering into the magnetic saturation state.

6) INTELLIGENT CONTROL

Considering the intelligent control has a strong self-learning and adaptive ability, it can be used for offline or online current optimization to reduce the torque ripple of SRMs, mainly including fuzzy logic, genetic algorithm, and neural network techniques.
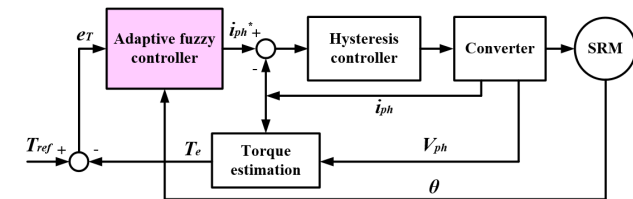

FIGURE 15. Adaptive fuzzy control for torque control of SRM [89].

Fig. 15 shows the block diagram of the adaptive fuzzy control for the SRM torque control [89]. The rotor position and phase currents are employed as the input and output for the controller, respectively. The instantaneous torque is estimated from a robust torque estimator which is used to determine the membership distribution of the adaptive fuzzy controller. The scheme does not rely on machine characteristics, and thus adapts to any change in motor characteristics. The controller can generate a smooth torque over the rated speed and is robust to errors presented in the rotor position, avoiding the negative torque in the phase commutation region and increasing the torque density. The adaptive fuzzy controller is designed in [90] for a four-phase SRM under faulty conditions. The torque can be easily controlled with a low torque ripple although faults happen including one-phase and two-phase open-circuit faults, providing a high-performance SRM drive with fault-tolerant ability.

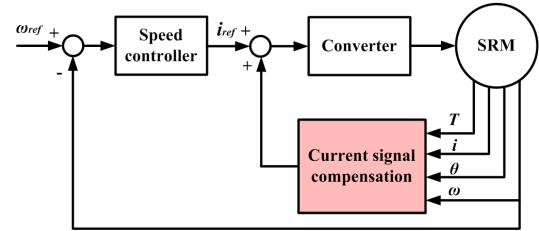A neuro-fuzzy compensation scheme is employed in [91] to constantly adjust the current compensation signal to

optimize the phase currents according to the torque, current, rotor position, and speed for torque ripple suppression. The block diagram of the compensation scheme is presented in Fig. 16. However, the estimated torque for the torque control implementation deteriorates the robustness and limits the application of control algorithms. Considering this point, an offline current modulation method by employing a neuro-fuzzy compensation is proposed in [92] for torque ripple reduction. An obvious advantage is that the torque signal is not required in this technique and the scheme can be applied for different speeds and loads.

A cerebellar model articulation controller based on neural network is employed to learning control in SRMs for torque ripple minimization in [93]. The desirable current profiles can be obtained by selecting the learning rate function under proper turn-on and turn-off angles during the network training process. The scheme provides a low torque ripple with a high power efficiency and offers a fast learning convergence in the system adaptation, which is adapted to a wide speed range. In [94], a novel multi-objective optimization scheme based on a genetic algorithm is presented for SRM drives, considering performance improvements of the low torque ripple and high efficiency. It shows that the torque ripple can be reduced by the optimal design method.

C. COMPARISON OF TORQUE RIPPLE REDUCTION TECHNIQUES

The comparison of torque ripple reduction techniques is illustrated in Table 2. The aforementioned motor topology design methods and control strategies are also summarized in terms of their adopted techniques, main advantages, and disadvantages. The first three methods in the table focus on motor topology improvements and the others are developed control schemes.

A higher number of rotor poles and also the pole shape design can effectively reduce the torque ripple and enhance the motor efficiency. The possible rotor shape design on pole arc, pole shoe, and nonuniform air gap have been investigated with a series of new motor structures proposed in recent years. For the control schemes, current and angle modulations are more easy to implement, while the torque ripple cannot be flexibly controlled for a wide speed range. The TSF based scheme is a favorable approach for the torque ripple reduction in SRMs, due to the optional TSF profiles. The i-T-θ characteristic of the motor should be previously obtained to

TABLE 2. Summary and comparison of torque ripple reduction techniques.

Method	Adopted technique	Advantage	Disadvantage	Reference
High number of rotor poles	Design the rotor with more pole number	Increased average torque; reduced torque ripple in non-saturation condition; reduced copper loss	Complicated rotor configuration; increased rotor materials	[44]-[46]
Pole shape design	Modification for desired rotor shapes, including pole arc, pole shoe and nonuniform air gap	Lower torque ripple; increased efficiency; high-speed operation performance	Complicated optimization for offline calculation	[48]-[55]
Current and angle modulation	Optimize the turn-on and turn-off angles or find required current profiles	Improved efficiency; enhanced torque-speed capability; lower torque ripple; realized easily	Current and torque cannot be flexibly controlled/need a large memory to store current profiles	[56]-[63]
ATC and DTC	Regulate torque by a hysteresis controller with online torque estimation	Direct controlled instantaneous torque; reduced torque ripple at a desired level	Need priori-knowledge of machine parameters	[64]-[72]
TSF based method	Definition of TSF profiles; implement hysteresis control with current reference derived from the torque reference	Easily controlled torque; determined torque waveforms; smooth torque over a wide speed range	Need i-T-θ characteristics; offline designed torque waveforms	[73]-[81]
FBL control	Transform the nonlinear system model into linear model	Reduced torque ripple; no nonlinear terms in feedback loop; provide required decoupling among currents	Not adapt to the change of uncertain parameters; complex linearization algorithm	[82]-[85]
ILC	Add a compensation current to the phase current reference for current tracking	No need to identify the system parameters; achieve perfect current tracking under different operation conditions	Complex learning control law; restriction of iteration cycle; degraded performance to transients	[86]-[88]
Intelligent control	Used for offline or online optimization of phase currents	Strong self-learning; adaptive ability; reduced torque ripple; no rely on machine parameters	Complex computational algorithm	[89]-[94]

implement this scheme. A smooth torque can be generated over a wide speed range if the actual current perfectly tracks the reference that derived from the TSF profiles. Therefore, the definition of the proper TSF profiles is the key point in this technique. FBL control, ILC, and intelligent control have been employed and developed for the purpose of torque ripple reduction. However, they have complicated algorithms.

D. TORQUE RIPPLE MINIMIZATION UNDER FAULTY CONDITIONS

The power converter is important in the motor system, where power switches are the most susceptible parts to fails, such as open-circuit and short-circuit faults. Although the asymmetric converters have the fault-tolerant ability, these faults still deteriorate the performance of the motor drives, especially the torque ripple and torque ability. Therefore, this section presents the torque ripple reduction technique under faulty conditions. Although the adaptive fuzzy controller in [90] and current profiling method in [95] can be used to mitigate the torque ripple in open-circuit fault conditions, the torque ripple is still much larger than that in the normal conditions.

Fig. 18 shows the fault-tolerant converter topology for SRMs proposed by Hu *et al.* [96], which can operate with

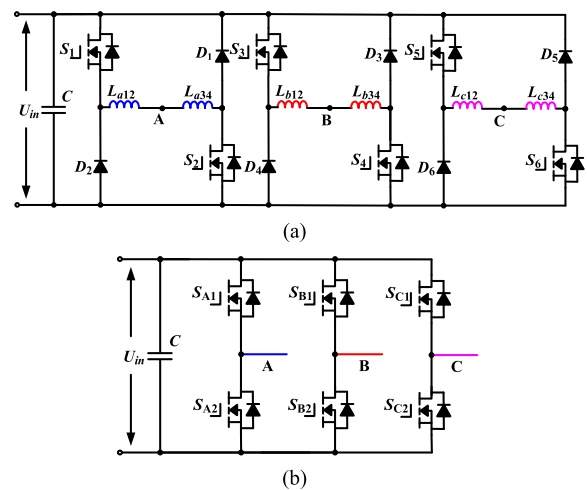**FIGURE 17.** Fault tolerant converter for SRMs [96]. (a) Conventional asymmetric converter. (b) Fault-tolerant module.

no torque ripple increase under faulty conditions. The central tapped nodes A, B and C of all the phases are developed in Fig. 17(a). The fault-tolerant module is a traditional three-phase inverter module, as shown in Fig. 17(b). The central nodes of the inverter are connected to the corresponding
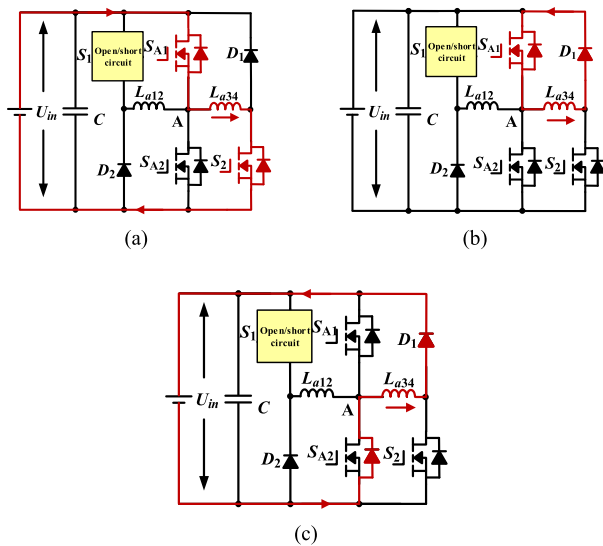
FIGURE 18. Fault-tolerant operation modes. (a) Excitation mode. (b) Freewheeling mode. (c) Energy recycling mode.

central tapped nodes of the three-phase windings. In healthy conditions, the drive topology works as a conventional asymmetric converter, where the fault-tolerant module is in the idle state. The fault-tolerant module is only put into use in faulty conditions, including open-circuit and short-circuit faults.

Fig. 18 shows the example of the switch S_1 under the open- or short-circuit condition. The half bridge converter with S_{A1} and S_{A2} is activated to combine the right part of the phase A converter to construct a new one, which can bypass the faulty part. The working modes of the fault-tolerant converter are similar to the traditional one, where the only difference is that a half phase winding is energized.

V. CONCLUSION AND FURTHER WORK

EVs and hybrid EVs have received increasing attention to reducing the fossil energy consumption and carbon-dioxide emissions. SRMs are gaining much interest for EVs and hybrid EVs due to the simple and robust structure, high reliability, and rare-earth-free feature. However, the acoustic noise problem caused by its inherent structure restricts further developments.

For high-performance vehicle applications, it is very important and urgent to optimize the SRM system to reduce the noise and vibration. To present clear solutions to the noise reduction in SRMs, this paper first gives a detailed analysis on the radial and tangential forces to explain the mechanism of the SRM noise, and then reviews the current state-of-the-art techniques to mitigate the radial vibration and torque ripple for the acoustic noise reduction. It concentrates on two aspects, including the motor topology optimization and control strategy improvement. The adopted methods, advantages, and limitations of these schemes are summarized and compared in details. Furthermore, the techniques that have been proposed by the authors are also presented and

discussed, including the motor pole skewing scheme, online TSF compensation method, and central-tapped converter topology. Therefore, this paper presents advanced solutions for the performance improvements to achieve low-noise SRM drives in EV applications.

From the review results, it can be found that many efforts have been made to optimize the motor topology by designing the new stator and rotor. However, the structure complexity and production cost are increased. Compared to the motor topology design, improving the control strategy is a more cost-effective and flexible way to deal with the acoustic noise in SRMs. Although the radial vibration and torque ripple can be significantly reduced by current methods, other performances such as torque and efficiency are reduced. Also, existing control strategies mainly focus on either low-speed or high-speed operations, while the noise and vibration reductions over a wide speed range have not been effectively achieved.

Therefore, future research works and forecast research hotspots are provided as follows.

1) The radial vibration and torque ripple of SRMs should be significantly reduced without obvious torque decline and efficiency decrease.

2) The low-noise SRM drive should be achieved by developing the motor topology without much change on the stator and rotor structures, where the fabrication complexity and production cost can be reduced.

3) Control schemes to reduce the radial vibration and torque ripple should be further developed for a wide speed range.

4) Torque ripple reduction techniques under converter fault conditions including open- and short-circuit faults should be developed by utilizing fewer additional power switches.

REFERENCES

[1] X. Hu, J. Jiang, B. Egardt, and D. Cao, "Advanced power-source integration in hybrid electric vehicles: Multicriteria optimization approach," *IEEE Trans. Ind. Electron.*, vol. 62, no. 12, pp. 7847–7858, Dec. 2015.

[2] C. Gan, N. Jin, Q. Sun, W. Kong, Y. Hu, and L. M. Tolbert, "Multiport bidirectional SRM drives for solar-assisted hybrid electric bus powertrain with flexible driving and self-charging functions," *IEEE Trans. Power Electron.*, to be published.

[3] L. Dang, N. Bernard, N. Bracikowski, and G. Berthiau, "Design optimization with flux weakening of high-speed PMSM for electrical vehicle considering the driving cycle," *IEEE Trans. Ind. Electron.*, vol. 64, no. 12, pp. 9834–9843, Dec. 2017.

[4] D. Fodorean, L. Idoumghar, M. Brévilliers, P. Minciunescu, and C. Irimia, "Hybrid differential evolution algorithm employed for the optimum design of a high-speed PMSM used for EV propulsion," *IEEE Trans. Ind. Electron.*, vol. 64, no. 12, pp. 9824–9833, Dec. 2017.

[5] L. Chen, G. Götting, and I. Hahn, "DC-link current and torque ripple optimized self-sensing control of interior permanent-magnet synchronous machines for hybrid and electrical vehicles," *IEEE Trans. Ind. Appl.*, vol. 53, no. 5, pp. 4536–4546, Sep./Oct. 2017.

[6] I. Boldea, L. N. Tutelea, L. Parsa, and D. Dorrell, "Automotive electric propulsion systems with reduced or no permanent magnets: An overview," *IEEE Trans. Ind. Electron.*, vol. 61, no. 10, pp. 5696–5711, Oct. 2014.

[7] S. Morimoto, S. Ooi, Y. Inoue, and M. Sanada, "Experimental evaluation of a rare-earth-free PMASynRM with ferrite magnets for automotive applications," *IEEE Trans. Ind. Electron.*, vol. 61, no. 10, pp. 5749–5756, Oct. 2014.

[8] E. Bostanci, M. Moallem, A. Parsapour, and B. Fahimi, "Opportunities and challenges of switched reluctance motor drives for electric propulsion: A comparative study," *IEEE Trans. Transport. Electrific.*, vol. 3, no. 1, pp. 58–75, Mar. 2017.

[9] W. Ding, S. Yang, Y. Hu, S. Li, T. Wang, and Z. Yin, "Design consideration and evaluation of a 12/8 high-torque modular-stator hybrid excitation switched reluctance machine for EV applications," *IEEE Trans. Ind. Electron.*, vol. 64, no. 12, pp. 9221–9232, Dec. 2017.

[10] W. Ding, H. Fu, and Y. Hu, "Characteristics assessment and comparative study of a segmented-stator permanent-magnet hybrid-excitation SRM drive with high-torque capability," *IEEE Trans. Ind. Electron.*, vol. 33, no. 1, pp. 482–500, Jan. 2018.

[11] J. Cai and Z. Deng, "Unbalanced phase inductance adaptable rotor position sensorless scheme for switched reluctance motor," *IEEE Trans. Power Electron.*, vol. 33, no. 5, pp. 4285–4292, May 2018.

[12] S. Song, Z. Xia, Z. Zhang, and W. Liu, "Control performance analysis and improvement of a modular power converter for three-phase SRM with Y-connected windings and neutral line," *IEEE Trans. Ind. Electron.*, vol. 63, no. 10, pp. 6020–6030, Oct. 2016.

[13] S. Song, Z. Xia, G. Fang, R. Ma, and W. Liu, "Phase current reconstruction and control of 3-phase switched reluctance machine with modular power converter using single DC-link current sensor," *IEEE Trans. Power Electron.*, to be published.

[14] A. Chiba, K. Kiyota, N. Hoshi, M. Takemoto, and S. Ogasawara, "Development of a rare-earth-free SR motor with high torque density for hybrid vehicles," *IEEE Trans. Energy Convers.*, vol. 30, no. 1, pp. 175–182, Mar. 2015.

[15] F. Peng, J. Ye, and A. Emadi, "An asymmetric three-level neutral point diode clamped converter for switched reluctance motor drives," *IEEE Trans. Power Electron.*, vol. 32, no. 11, pp. 8618–8631, Nov. 2017.

[16] F. Yi and W. Cai, "Modeling, control, and seamless transition of the bidirectional battery-driven switched reluctance motor/generator drive based on integrated multiport power converter for electric vehicle applications," *IEEE Trans. Power Electron.*, vol. 31, no. 10, pp. 7099–7111, Oct. 2016.

[17] C. Gan, J. Wu, S. Yang, and Y. Hu, "Phase current reconstruction of switched reluctance motors from DC-link current under double high-frequency pulses injection," *IEEE Trans. Ind. Electron.*, vol. 62, no. 5, pp. 3265–3276, May 2015.

[18] C. Gan, J. Wu, Y. Hu, S. Yang, W. Cao, and J. M. Guerrero, "New integrated multilevel converter for switched reluctance motor drives in plug-in hybrid electric vehicles with flexible energy conversion," *IEEE Trans. Power Electron.*, vol. 32, no. 5, pp. 3754–3766, May 2017.

[19] V. Valdivia, R. Todd, F. J. Bryan, A. Barrado, A. Lazaro, and A. J. Forsyth, "Behavioral modeling of a switched reluctance generator for aircraft power systems," *IEEE Trans. Ind. Electron.*, vol. 61, no. 6, pp. 2690–2699, Jun. 2014.

[20] H. Chen and J. J. Gu, "Implementation of the three-phase switched reluctance machine system for motors and generators," *IEEE/ASME Trans. Mechatronics*, vol. 15, no. 3, pp. 421–432, Jun. 2010.

[21] D. Wang, X. Du, D. Zhang, and X. Wang, "Design, optimization, and prototyping of segmental-type linear switched-reluctance motor with a toroidally wound mover for vertical propulsion application," *IEEE Trans. Ind. Electron.*, vol. 65, no. 2, pp. 1865–1874, Feb. 2018.

[22] C. Lin and B. Fahimi, "Prediction of radial vibration in switched reluctance machines," *IEEE Trans. Energy Convers.*, vol. 28, no. 4, pp. 1072–1081, Dec. 2013.

[23] C. Lin and B. Fahimi, "Prediction of acoustic noise in switched reluctance motor drives," *IEEE Trans. Energy Convers.*, vol. 29, no. 1, pp. 250–258, Mar. 2014.

[24] M. N. Anwar and O. Husain, "Radial force calculation and acoustic noise prediction in switched reluctance machines," *IEEE Trans. Ind. Appl.*, vol. 36, no. 6, pp. 1589–1597, Nov. 2000.

[25] I. Husain, A. Radun, and J. Nairus, "Unbalanced force calculation in switched-reluctance machines," *IEEE Trans. Magn.*, vol. 36, no. 1, pp. 330–338, Jan. 2000.

[26] Z. Tang, P. Pillay, Y. Chen, and A. M. Omekanda, "Prediction of electromagnetic forces and vibrations in SRMs operating at steady-state and transient speeds," *IEEE Trans. Ind. Appl.*, vol. 41, no. 4, pp. 927–934, Jul./Aug. 2005.

[27] X. Guo, R. Zhong, M. Zhang, D. Ding, and W. Sun, "Fast computation of radial vibration in switched reluctance motors," *IEEE Trans. Ind. Electron.*, vol. 65, no. 6, pp. 4588–4598, Jun. 2018.

[28] P. O. Rasmussen, J. H. Andreasen, and J. M. Pijanowski, "Structural stator spacers-a solution for noise reduction of switched reluctance motors," *IEEE Trans. Ind. Appl.*, vol. 40, no. 2, pp. 574–581, Mar./Apr. 2004.

[29] K. Kiyota, T. Kakishima, A. Chiba, and M. A. Rahman, "Cylindrical rotor design for acoustic noise and windage loss reduction in switched reluctance motor for HEV applications," *IEEE Trans. Ind. Appl.*, vol. 52, no. 1, pp. 154–162, Jan./Feb. 2016.

[30] J. Li and Y. Cho, "Investigation into reduction of vibration and acoustic noise in switched reluctance motors in radial force excitation and frame transfer function aspects," *IEEE Trans. Magn.*, vol. 45, no. 10, pp. 4664–4667, Oct. 2009.

[31] S. M. Castano, B. Bilgin, E. Fairall, and A. Emadi, "Acoustic noise analysis of a high-speed high-power switched reluctance machine: Frame effects," *IEEE Trans. Energy Convers.*, vol. 31, no. 31, pp. 69–77, Mar. 2016.

[32] M. Abbasian, M. Moallem, and B. Fahimi, "Double-stator switched reluctance machines (DSSRM): Fundamentals and magnetic force analysis," *IEEE Trans. Energy Convers.*, vol. 25, no. 3, pp. 589–597, Sep. 2010.

[33] A. H. Isfahani and B. Fahimi, "Comparison of mechanical vibration between a double-stator switched reluctance machine and a conventional switched reluctance machine," *IEEE Trans. Magn.*, vol. 50, no. 2, pp. 293–296, Feb. 2014.

[34] H. Yang, Y. Lim, and H. Kim, "Acoustic noise/vibration reduction of a single-phase SRM using skewed stator and rotor," *IEEE Trans. Ind. Elect.*, vol. 60, no. 10, pp. 4292–4300, Oct. 2013.

[35] Y. Zou, K. W. E. Cheng, N. C. Cheung, and J. Pan, "Deformation and noise mitigation for the linear switched reluctance motor with skewed teeth structure," *IEEE Trans. Magn.*, vol. 50, no. 11, pp. 1–4, Nov. 2014.

[36] C. Gan, J. Wu, M. Shen, S. Yang, Y. Hu, and W. Cao, "Investigation of skewing effects on the vibration reduction of three-phase switched reluctance motors," *IEEE Trans. Magn.*, vol. 51, no. 9, Sep. 2015, Art. no. 8203509.

[37] F. C. Lin and S. M. Yang, "An approach to producing controlled radial force in a switched reluctance motor," *IEEE Trans. Ind. Electron.*, vol. 54, no. 4, pp. 2137–2146, Aug. 2007.

[38] F. C. Lin and S. M. Yang, "Instantaneous shaft radial force control with sinusoidal excitations for switched reluctance motors," *IEEE Trans. Energy Convers.*, vol. 22, no. 3, pp. 629–636, Sep. 2007.

[39] J.-W. Ahn, S.-J. Park, and D.-H. Lee, "Hybrid excitation of SRM for reduction of vibration and acoustic noise," *IEEE Trans. Ind. Electron.*, vol. 51, no. 2, pp. 374–380, Apr. 2004.

[40] X. Cao, Z. Deng, G. Yang, and X. Wang, "Independent control of average torque and radial force in bearingless switched-reluctance motors with hybrid excitations," *IEEE Trans. Power Electron.*, vol. 24, no. 5, pp. 1376–1385, May 2009.

[41] C. Pollock and C.-Y. Wu, "Acoustic noise cancellation techniques for switched reluctance drives," *IEEE Trans. Ind. Appl.*, vol. 33, no. 2, pp. 477–484, Mar. 1997.

[42] Z. Q. Zhu, X. Liu, and Z. Pan, "Analytical model for predicting maximum reduction levels of vibration and noise in switched reluctance machine by active vibration cancellation," *IEEE Trans. Energy Convers.*, vol. 26, no. 1, pp. 36–45, Mar. 2011.

[43] H. Makino, T. Kosaka, and N. Matsui, "Digital PWM-control-based active vibration cancellation for switched reluctance motors," *IEEE Trans. Ind. Appl.*, vol. 51, no. 6, pp. 4521–4530, Nov./Dec. 2015.

[44] P. C. Desai, M. Krishnamurthy, N. Schofield, and A. Emadi, "Novel switched reluctance machine configuration with higher number of rotor poles than stator poles: Concept to implementation," *IEEE Trans. Ind. Electron.*, vol. 57, no. 2, pp. 649–659, Feb. 2010.

[45] B. Bilgin, A. Emadi, and M. Krishnamurthy, "Design considerations for switched reluctance machines with a higher number of rotor poles," *IEEE Trans. Ind. Electron.*, vol. 59, no. 10, pp. 3745–3756, Oct. 2012.

[46] X. Liu and Z. Q. Zhu, "Stator/rotor pole combinations and winding configurations of variable flux reluctance machines," *IEEE Trans. Ind. Appl.*, vol. 50, no. 6, pp. 3675–3684, Nov. 2014.

[47] T. J. E. Miller, *Switched Reluctance Motors and Their Control*. Oxford, U.K.: Magna Phys Publ, 1993.

[48] N. K. Sheth and K. R. Rajagopal, "Optimum pole arcs for a switched reluctance motor for higher torque with reduced ripple," *IEEE Trans. Magn.*, vol. 39, no. 5, pp. 3214–3216, Sep. 2003.

[49] J. W. Lee, H. S. Kim, B. I. Kwon, and B. T. Kim, "New rotor shape design for minimum torque ripple of SRM using FEM," *IEEE Trans. Magn.*, vol. 40, no. 2, pp. 754–757, Mar. 2004.

[50] N. K. Sheth and K. R. Rajagopal, "Torque profiles of a switched reluctance motor having special pole face shapes and asymmetric stator poles," *IEEE Trans. Magn.*, vol. 40, no. 4, pp. 2035–2037, Jul. 2004.

[51] Y. K. Choi, H. S. Yoon, and C. S. Koh, "Pole-shape optimization of a switched-reluctance motor for torque ripple reduction," *IEEE Trans. Magn.*, vol. 43, no. 4, pp. 1797–1800, Apr. 2007.

[52] J. W. Jiang, B. Bilgin, and A. Emadi, "Three-phase 24/16 switched reluctance machine for a hybrid electric powertrain," *IEEE Trans. Transport. Electrific.*, vol. 3, no. 1, pp. 76–85, Mar. 2017.

[53] G. Li, J. Ojeda, S. Hlioui, E. Hoang, M. Lecrivain, and M. Gabsi, "Modification in rotor pole geometry of mutually coupled switched reluctance machine for torque ripple mitigating," *IEEE Trans. Magn.*, vol. 48, no. 6, pp. 2025–2034, Jun. 2012.

[54] C. Sahin, A. E. Amac, M. Karacor, and A. Emadi, "Reducing torque ripple of switched reluctance machines by relocation of rotor moulding clinches," *IET Electr. Power Appl.*, vol. 6, no. 9, pp. 753–760, Nov. 2012.

[55] D. H. Lee, T. H. Pham, and J. W. Ahn, "design and operation characteristics of four-two pole high-speed SRM for torque ripple reduction," *IEEE Trans. Ind. Electron.*, vol. 60, no. 9, pp. 3637–3643, Sep. 2013.

[56] P. C. Kjaer, J. J. Gribble, and T. J. E. Miller, "High-grade control of switched reluctance machines," *IEEE Trans. Ind. Appl.*, vol. 33, no. 6, pp. 1585–1593, Nov. 1997.

[57] C. Mademlis and I. Kioskeridis, "Performance optimization in switched reluctance motor drives with online commutation angle control," *IEEE Trans. Energy Convers.*, vol. 18, no. 3, pp. 448–457, Sep. 2003.

[58] X. D. Xue *et al.*, "Optimal control method of motoring operation for SRM drives in electric vehicles," *IEEE Trans. Veh. Technol.*, vol. 59, no. 3, pp. 1191–1204, Mar. 2010.

[59] R. Gobbi and K. Ramar, "Optimisation techniques for a hysteresis current controller to minimise torque ripple in switched reluctance motors," *IET Electr. Power Appl.*, vol. 3, no. 5, pp. 453–460, Sep. 2009.

[60] N. T. Shaked and R. Rabinovici, "New procedures for minimizing the torque ripple in switched reluctance motors by optimizing the phase-current profile," *IEEE Trans. Magn.*, vol. 41, no. 3, pp. 1184–1192, Mar. 2005.

[61] R. Mikail, I. Husain, Y. Sozer, M. S. Islam, and T. Sebastian, "Torque-ripple minimization of switched reluctance machines through current profiling," *IEEE Trans. Ind. Appl.*, vol. 49, no. 3, pp. 1258–1267, May 2013.

[62] R. Mikail, I. Husain, M. S. Islam, Y. Sozer, and T. Sebastian, "Four-quadrant torque ripple minimization of switched reluctance machine through current profiling with mitigation of rotor eccentricity problem and sensor errors," *IEEE Trans. Ind. Appl.*, vol. 51, no. 3, pp. 2097–2104, May/Jun. 2015.

[63] Z. Lin, D. Reay, B. Williams, and X. He, "High-performance current control for switched reluctance motors based on on-line estimated parameters," *IET Electr. Power Appl.*, vol. 4, no. 1, pp. 67–74, Jan. 2010.

[64] R. B. Inderka and R. W. A. A. D. Doncker, "High-dynamic direct average torque control for switched reluctance drives," *IEEE Trans. Ind. Appl.*, vol. 39, no. 4, pp. 1040–1045, Jul. 2003.

[65] I. Husain, "Minimization of torque ripple in SRM drives," *IEEE Trans. Ind. Electron.*, vol. 49, no. 1, pp. 28–39, Feb. 2002.

[66] A. D. Cheok and Y. Fukuda, "A new torque and flux control method for switched reluctance motor drives," *IEEE Trans. Power Electron.*, vol. 17, no. 4, pp. 543–557, Jul. 2002.

[67] I. Husain and M. Ehsani, "Torque ripple minimization in switched reluctance motor drives by PWM current control," *IEEE Trans. Power Electron.*, vol. 11, no. 1, pp. 83–88, Jan. 1996.

[68] R. B. Inderka and R. W. A. A. De Doncker, "DITC—Direct instantaneous torque control of switched reluctance drives," *IEEE Trans. Ind. Appl.*, vol. 39, no. 4, pp. 1046–1051, Jul. 2003.

[69] N. H. Fuengwarodsakul, M. Menne, R. B. Inderka, and R. W. De Doncker, "High-dynamic four-quadrant switched reluctance drive based on DITC," *IEEE Trans. Ind. Appl.*, vol. 41, no. 5, pp. 1232–1242, Sep. 2005.

[70] A. Klein-Hessling, A. Hofmann, and R. W. De Doncker, "Direct instantaneous torque and force control: A control approach for switched reluctance machines," *IET Electr. Power Appl.*, vol. 11, no. 5, pp. 935–943, May 2017.

[71] K. F. Wong, K. W. E. Cheng, and S. L. Ho, "On-line instantaneous torque control of a switched reluctance motor based on co-energy control," *IET Electr. Power Appl.*, vol. 3, no. 4, pp. 257–264, Jul. 2009.

[72] S. K. Sahoo, S. Dasgupta, S. K. Panda, and J.-X. Xu, "A Lyapunov function-based robust direct torque controller for a switched reluctance motor drive system," *IEEE Trans. Power Electron.*, vol. 27, no. 2, pp. 555–564, Feb. 2012.

[73] V. P. Vujičić, "Minimization of torque ripple and copper losses in switched reluctance drive," *IEEE Trans. Power Electron.*, vol. 27, no. 1, pp. 388–399, Jan. 2012.

[74] C.-H. Kim and I.-J. Ha, "A new approach to feedback-linearizing control of variable reluctance motors for direct-drive applications," *IEEE Trans. Control Syst. Technol.*, vol. 4, no. 4, pp. 348–362, Jul. 1996.

[75] C. Choi, S. Kim, Y. Kim, and K. Park, "A new torque control method of a switched reluctance motor using a torque-sharing function," *IEEE Trans. Magn.*, vol. 38, no. 5, pp. 3288–3290, Sep. 2002.

[76] D. H. Lee, J. Liang, Z. G. Lee, and J. W. Ahn, "A simple nonlinear logical torque sharing function for low-torque ripple SR drive," *IEEE Trans. Ind. Electron.*, vol. 56, no. 8, pp. 3021–3028, Aug. 2009.

[77] X. D. Xue, K. W. E. Cheng, and S. L. Ho, "Optimization and evaluation of torque-sharing functions for torque ripple minimization in switched reluctance motor drives," *IEEE Trans. Power Electron.*, vol. 24, no. 9, pp. 2076–2090, Sep. 2009.

[78] H. J. Brauer, M. D. Hennen, and R. W. De Doncker, "Control for polyphase switched reluctance machines to minimize torque ripple and decrease ohmic machine losses," *IEEE Trans. Power Electron.*, vol. 27, no. 1, pp. 370–378, Jan. 2012.

[79] J. Ye, B. Bilgin, and A. Emadi, "An extended-speed low-ripple torque control of switched reluctance motor drives," *IEEE Trans. Power Electron.*, vol. 30, no. 3, pp. 1457–1470, Mar. 2015.

[80] J. Ye, B. Bilgin, and A. Emadi, "An offline torque sharing function for torque ripple reduction in switched reluctance motor drives," *IEEE Trans. Energy Convers.*, vol. 30, no. 2, pp. 726–735, Jun. 2015.

[81] Q. Sun, J. Wu, C. Gan, Y. Hu, and J. Si, "OCTSF for torque ripple minimisation in SRMs," *IET Power Electron.*, vol. 9, no. 14, pp. 2741–2750, Sep. 2016.

[82] M. Ilic'-Spong, R. Marino, S. M. Peresada, and D. Taylor, "Feedback linearizing control of switched reluctance motors," *IEEE Trans. Autom. Control*, vol. 32, no. 5, pp. 371–379, May 1987.

[83] S. K. Panda and P. K. Dash, "Application of nonlinear control to switched reluctance motors: A feedback linearisation approach," *IEE Proc.-Electr. Power Appl.*, vol. 143, no. 5, pp. 371–379, Sep. 1996.

[84] S. A. Bortoff, R. R. Kohan, and R. Milman, "Adaptive control of variable reluctance motors: A spline function approach," *IEEE Trans. Ind. Electron.*, vol. 45, no. 3, pp. 433–444, Jun. 1998.

[85] H.-K. Bae and R. Krishnan, "A novel approach to control of switched reluctance motors considering mutual inductance," in *Proc. IEEE 26th Annu. Conf. Ind. Electron. Soc. (IECON)*, Oct. 2000, pp. 369–374.

[86] N. C. Sahoo, J. X. Xu, and S. K. Panda, "Low torque ripple control of switched reluctance motors using iterative learning," *IEEE Trans. Energy Convers.*, vol. 16, no. 4, pp. 318–326, Dec. 2001.

[87] S. K. Sahoo, S. K. Panda, and J. X. Xu, "Iterative learning-based high-performance current controller for switched reluctance motors," *IEEE Trans. Energy Convers.*, vol. 19, no. 3, pp. 491–498, Sep. 2004.

[88] S. K. Sahoo, S. K. Panda, and J.-X. Xu, "Indirect torque control of switched reluctance motors using iterative learning control," *IEEE Trans. Power Electron.*, vol. 20, no. 1, pp. 200–208, Jan. 2005.

[89] S. Mir, M. E. Elbuluk, and I. Husain, "Torque-ripple minimization in switched reluctance motors using adaptive fuzzy control," *IEEE Trans. Ind. Appl.*, vol. 35, no. 2, pp. 461–468, Mar. 1999.

[90] S. Mir, M. S. Islam, T. Sebastian, and I. Husain, "Fault-tolerant switched reluctance motor drive using adaptive fuzzy logic controller," *IEEE Trans. Power Electron.*, vol. 19, no. 2, pp. 289–295, Mar. 2004.

[91] L. O. A. P. Henriques, L. G. B. Rolim, W. I. Suemitsu, P. J. C. Branco, and J. A. Dente, "Torque ripple minimization in a switched reluctance drive by neuro-fuzzy compensation," *IEEE Trans. Magn.*, vol. 36, no. 5, pp. 3592–3594, Sep. 2000.

[92] L. O. A. P. Henriques, P. J. C. Branco, L. G. B. Rolim, and W. I. Suemitsu, "Proposition of an offline learning current modulation for torque-ripple reduction in switched reluctance motors: Design and experimental evaluation," *IEEE Trans. Ind. Electron.*, vol. 49, no. 3, pp. 665–676, Jun. 2002.

[93] C. Shang, D. Reay, and B. Williams, "Adapting CMAC neural networks with constrained LMS algorithm for efficient torque ripple reduction in switched reluctance motors," *IEEE Trans. Control Syst. Technol.*, vol. 7, no. 4, pp. 401–413, Jul. 1999.

[94] B. Mirzaeian, M. Moallem, V. Tahani, and C. Lucas, "Multiobjective optimization method based on a genetic algorithm for switched reluctance motor design," *IEEE Trans. Magn.*, vol. 38, no. 3, pp. 1524–1527, May 2002.

[95] P. Dúbravka, P. Rafajdus, P. Makyš, and L. Szabó, "Control of switched reluctance motor by current profiling under normal and open phase operating condition," *IET Electr. Power Appl.*, vol. 11, no. 4, pp. 548–556, Apr. 2017.

[96] Y. Hu, C. Gan, W. Cao, W. Li, and S. J. Finney, "Central-tapped node linked modular fault-tolerance topology for SRM applications," *IEEE Trans. Power Electron.*, vol. 31, no. 2, pp. 1541–1554, Feb. 2016.

CHUN GAN (S'14–M'16) received the B.S. and M.S. degrees in power electronics and motor drives from the China University of Mining and Technology, Xuzhou, China, in 2009 and 2012, respectively, and the Ph.D. degree in power electronics and motor drives from Zhejiang University, Hangzhou, China, in 2016.

He is currently a Research Associate with the Department of Electrical Engineering and Computer Science, The University of Tennessee, Knoxville, TN, USA. He has published over 50 technical papers in leading journals and conference proceedings, including over 20 IEEE Transaction papers. He has 12 issued/published invention patents. His research interests include high-efficiency power converters, electric vehicles, electrical motor drives, electrical motor design, continuous variable series reactors, high-voltage direct current transmission, and microgrids.

Dr. Gan received the 2018 Marie Sklodowska-Curie Actions Seal of Excellence from the European Commission, the 2015 Top Ten Excellent Scholar Award, the 2016 Excellent Ph.D. Graduate Award, the 2015 Ph.D. National Scholarship, the 2015 Wang Guosong Scholarship, and the 2014 and 2015 Outstanding Ph.D. Candidate Awards in Zhejiang University.

JIANHUA WU received the B.S. degree in electrical engineering from the Nanjing University of Aeronautics and Astronautics, China, and the M.S. and Ph.D. degrees in electrical engineering from the Huazhong University of Science and Technology, China, in 1983, 1991, and 1994, respectively.

From 1983 to 1989, he was with Guiyang Electric Company as a Design Engineer. Since 2005, he has been a Professor with the College of Electrical Engineering, Zhejiang University, China. He developed the motor design software Visual EMCAD, which is widely used in China. His research interests are electric machine design and drives, including switched reluctance motors and permanent magnet machines for electric vehicle applications.

Dr. Wu is serving as a member of the Electrical Steel of Chinese Society for Metals, the Small-Power Machine Committee of the China Electrotechnical Society, and the Standardization Administration of China.

QINGGUO SUN received the B.S. degree in electrical engineering from Qingdao University, Shandong, China, in 2014. He is currently pursuing the Ph.D. degree with the College of Electrical Engineering, Zhejiang University, Hangzhou, China.

His research interests include motor design and control in switched reluctance motor, particularly for the optimization of the torque ripple and efficiency of the motor system.
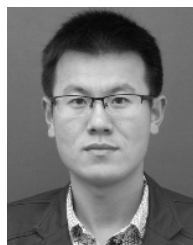
WUBIN KONG (M'15) received the B.S. and Ph.D. degrees from Zhejiang University, Hangzhou, China, in 2009 and 2014, respectively. Since 2015, he has been a Lecturer with the Huazhong University of Science and Technology, Wuhan, China. His research interests are high-power multiphase motor drives and fault tolerant control motor drive applied in EV.

HONGYU LI (S'14) received the B.S. degree in electrical engineering in 2012. He is currently pursuing the Ph.D. degree in electrical engineering with Hohai University, Nanjing, China. He is currently performing research with The University of Tennessee, Knoxville, TN, USA, as a Visiting Student.

His main research interests focus on renewable energy and power system dynamic analysis.

YIHUA HU (M'13–SM'15) received the B.S. degree in electrical motor drives and the Ph.D. degree in power electronics and drives from the China University of Mining and Technology, Xuzhou, China, in 2003 and 2011, respectively.

From 2011 to 2013, he was with the College of Electrical Engineering, Zhejiang University, as a Post-Doctoral Fellow. From 2012 to 2013, he was an Academic Visiting Scholar with the School of Electrical and Electronic Engineering, Newcastle University, Newcastle upon Tyne, U.K. From 2013 to 2015, he was a Research Associate with the Power Electronics and Motor Drive Group, University of Strathclyde. He is currently a Lecturer with the Department of Electrical Engineering and Electronics, University of Liverpool. He has published over 35 peer reviewed technical papers in leading journals. His research interests include PV generation system, power electronics converters and control, and electrical motor drives.

• • •